Technical Note: Noble gas extraction procedure and performance of the Cologne Helix MC Plus multi-collector noble gas mass spectrometer for cosmogenic neon isotope analysis

Benedikt Ritter[1*], Andreas Vogt[1], Tibor J. Dunai[1*]

[1] University of Cologne, Institute of Geology and Mineralogy, Zülpicher Straße 49b, Köln 50674, Germany

*Corresponding authors

Benedikt Ritter – benedikt.ritter@uni-koeln.de

Tibor J. Dunai – tdunai@uni-koeln.de

Keywords: Noble Gas, Mass Spectrometry, Cosmogenic Nuclides

Abstract:

We established a new laboratory for noble gas mass spectrometry that is dedicated to the development and application to cosmogenic nuclides at the University of Cologne (Germany). At the core of the laboratory are a state-of-the-art high mass resolution multicollector Helix MCPlus (Thermo-Fisher) noble gas mass spectrometer and a novel custom-designed automated extraction line. The mass spectrometer is equipped with five combined Faraday Multiplier collectors, with $10^{12}\,\Omega$ and $10^{13}\,\Omega$ pre-amplifiers for faraday collectors. We describe the extraction line and the automated procedure for cosmogenic neon and the current performance of the experimental setup. Performance tests were conducted using gas of atmospheric isotopic composition (our primary standard gas), as well as CREU-1 intercomparison material, containing a mixture of neon of atmospheric and cosmogenic composition. We use the results from repeated analysis of CREU-1 to assess the performance of the current experimental setup at Cologne. The precision in determining the abundance of cosmogenic ^{21}Ne is equal to or better than those reported for other laboratories. The absolute value we obtain for the concentration of cosmogenic ^{21}Ne in CREU is indistinguishable from the published value.

1. Introduction

Cosmogenic Ne isotopes are stable and compared to other cosmogenic radionuclides (e.g., ^{10}Be, ^{26}Al) exhibit the potential to date beyond the physical limit of radionuclides. The particular strength of cosmogenic neon is its application to date quartz clasts of very old surfaces (>4 Ma) or very slowly eroding landscapes (<10 cm/Ma), which is unattainable with most other radionuclides (Dunai, 2010). Cosmogenic Ne analysis can be applied to a range of neon-retentive minerals (e.g., quartz, olivine and pyroxene), amongst which quartz is the most commonly used. Ne can be measured on conventional sector field noble gas mass spectrometers, is less time consuming and requires less sample-preparation compared to AMS measurements required for

36 the cosmogenic radionuclides. Recent studies used cosmogenic Ne for dating old surfaces (e.g.

37 Ritter et al., 2018; Dunai et al., 2005; Binnie et al., 2020), reconstructing erosion rates (e.g. Ma et

38 al., 2016), or $^{10}Be/^{21}Ne$ burial dating (e.g. Mcphillips et al., 2016). The advantage to use also other

39 minerals than quartz, led to several studies using ^{21}Ne to date for example basalt flows (e.g.

40 Espanon et al., 2014; Gillen et al., 2010). Neon has three stable isotopes ^{20}Ne, ^{21}Ne, and ^{22}Ne, of

41 which ^{20}Ne is the most abundant; the atmospheric $^{21}Ne/^{20}Ne$ and $^{22}Ne/^{20}Ne$ ratios are 0.002959 ±

42 0.000022 and 0.1020 ± 0.0008, respectively (Eberhardt et al., 1965). There are several recent

43 re-determinations of the atmospheric $^{21}Ne/^{20}Ne$ ratio (e.g. Honda et al., 2015; Wielandt and

44 Storey, 2019; Saxton, 2020; Györe et al., 2019) one of which yields a ~2 % lower value (Honda et

45 al., 2015). For the evaluation of our data, we utilize the $^{21}Ne/^{20}Ne$ value of Wielandt and Storey

46 (2019) of 0.0029577 ± 0.0000014 and for $^{22}Ne/^{20}Ne$ that of Eberhardt et al. (1965). Note, that in

47 the context of the determination of the *abundance* of cosmogenic nuclides in a sample eventual

48 differences between the used and the actual value of the atmospheric $^{21}Ne/^{20}Ne$ ratio are

49 unimportant, if (i) atmospheric neon is used as calibration gas, (ii) the same value for the

50 composition of atmospheric neon is used consistently throughout the evaluation of the isotope

51 data (mass discrimination etc.) and calculation of abundances and (iii) the atmospheric value used

52 is reported along with the data.

53 All three neon isotopes are produced in about equal proportions by neutron spallation in quartz

54 (Niedermann et al., 1994). Due to the lower abundances of ^{21}Ne and ^{22}Ne as compared to ^{20}Ne in

55 air, and the ubiquitous presence of atmospheric neon in samples, any contribution from

56 cosmogenic production in samples is most easily picked up with the former two isotopes.

57 Consequently, the neon three-isotope diagram with ^{20}Ne as common denominator (Niedermann

58 et al., 1994; Niedermann, 2002) is customarily used to asses ^{21}Ne-data for the presence of

59 terrestrial cosmogenic Ne and its discrimination from other non-atmospheric Ne-components

60 (Dunai, 2010). The latter may be nucleonic Ne and/or mantle-derived Ne. Hence, the accurate

61 determination of cosmogenic Ne and its discrimination from other components requires the

62 accurate discrimination from any other component.

63 Common isobaric interferences for neon measurements are at: m/e = 20 ($^{40}Ar^{2+}$, $H^{19}F^+$ and $H_2^{18}O^+$

64 interfering with $^{20}Ne^+$), at m/e = 21 ($^{20}NeH^+$, interfering with $^{21}Ne^+$), and at m/e = 22 ($^{44}CO_2^{2+}$

65 interfering with $^{22}Ne^+$). $^{40}Ar^{2+}$ and $^{12}C^{16}O_2^{2+}$ interferences are considered to be the main challenges

66 for neon analysis. Recent studies demonstrated the ability of the Helix MCPlus to fully resolve the

67 $^{40}Ar^{2+}$, $H^{19}F^+$ and $H_2^{18}O^+$ peaks from the $^{20}Ne^+$ peak (e.g. Honda et al., 2015; Wielandt and Storey,

68 2019) and its ability to reliably measure ^{21}Ne at an off-centre peak position that is free of

69 interference from $^{20}NeH^+$ (Honda et al., 2015; Wielandt and Storey, 2019). The remaining

70 interference of $^{12}C^{16}O_2^{2+}$ at m/e = 22 can be corrected via monitoring of the double/single-charged

71 ratio of CO_2 in-between samples (Honda et al., 2015) or the measurement of $^{13}C^{16}O_2^{2+}$ at

72   m/e = 22.5 during sample analysis (Wielandt and Storey, 2019). Recently mass spectrometers

73   with higher resolution have become available, which permit almost full separation of $^{12}C^{16}O_2^{2+}$ and

74   ^{22}Ne (Farley et al., 2020).

75   Beside the resolution and characteristics of a noble gas mass spectrometer to resolve and

76   quantitatively determine neon compositions of an unknown sample, the calibration, sample

77   extraction and purification are crucial achieving accurate and reproducible results. Automation of

78   extraction protocols and workflows may assist in achieving a high degree of reproducibility by

79   eliminating inaccuracies or errors by operators having a variable degree of expertise. In this

80   paper, we describe the current setup of the noble gas mass spectrometer and its automated

81   extraction line that is located in the Institute of Geology and Mineralogy at the University of

82   Cologne (Germany), and we review its performance for neon analysis.

83   ## 2. Experimental setup

84   ### 2.1 Noble gas mass-spectrometer

85   The Cologne noble gas laboratory is equipped with a Helix MCPlus from Thermo Fisher Scientific

86   with five CFM modules (Combined Faraday Multiplier), called 'Aura'. The central, axial module

87   (Ax) is fixed in position, the four remaining modules (L1, L2 on the low mass side, and H1,

88   H2 on the high mass side of Ax) can be moved. The mass spectrometer configuration and

89   performance is mostly equivalent to those described elsewhere (Honda et al., 2015; Wielandt and

90   Storey, 2019); here we describe potential differences in configuration and performance

91   parameters that may be unique to a given instrument (Fig. 1).

92   In the instrument at Cologne University, all but one Faraday amplifier, are equipped with 10^{13} Ω

93   resistors, one with 10^{12} Ω (H2). The L1 module has 0.3 mm wide collector slits, all other modules

94   have 0.6 mm wide slits. The CFM at L1 configuration is flipped (i.e., the relative positions of the

95   Faraday and Multiplier are swapped) as compared to the standard configuration, which is the only

96   difference from the standard configuration. The two SAES NP10 getters, at the source and the

97   multiplier block, are kept at room temperature during analysis.

98   For neon isotope analysis of calibrations and samples, we utilize the H1, Ax and L1 CFMs ($^{20}Ne^+$

99   L1 Faraday; $^{22}Ne^+$ H1 Faraday; $^{21}Ne^+$ L1 multiplier; CO_2^+ H1 Faraday; for blanks we utilize the L1

100   multiplier also for $^{20}Ne^+$ and $^{22}Ne^{++}$). With the widest source slit (0.25 mm) mass resolution (at 5%

101   peak valley) and mass resolving power (between 10% and 90% of peak) on the L1 detector with

102   0.3 mm collector slit width are approximately 1700 and 6500, respectively. For the Ax and H1

103   detectors with 0.6 mm collector slit, the corresponding values are approximately 1000 and 6000,

104   respectively. As such the system allows the interference-free determination of ^{20}Ne and ^{21}Ne; for

105 [21]Ne this entails measuring at an off-centre peak position (Honda et al., 2015; Wielandt and Storey,
106 2019).

107 **2.2 Extraction line**

108 The Cologne noble gas extraction and purification line has a modular design. Modules are (i)
109 extraction (currently only laser extraction; to be joined by a crushing device), (ii) calibration gas
110 pipettes and volumes, (iii) clean-up, and (iv) cryogenic separation. The calibration module is
111 physically linked to the clean-up module, the other modules can be separated, if required. Among
112 the common features of all modules is that all valves and tubing in contact with the sample gas are
113 made of metal; tubing is of stainless steel or vacuum-annealed copper. Furthermore, all valves
114 used for handling of sample and calibration gas are pneumatically actuated all-metal diaphragm
115 valves (Fujikin MEGA-M LA; FWB(R)-71-6.35), that can be operated at high temperature (up to
116 350ºC). Tubing and valves in contact with sample gas are continuously kept at constant
117 temperature between 160 ºC and 200 ºC; exceptions are the functional traps and portions of the
118 tubing in the cryogenic separation. Temperature is maintained with heating tapes (Horst HS
119 450 ºC) and is controlled section-wise (Horst HT30). The temperature of the heated sections is
120 controlled to ±1 ºC. Thermal insulation is achieved with high-temperature resistant silicone foam
121 (HOKOSIL®; resists ≤280 ºC; permitting bake-out at higher than operation temperatures).
122 Vacuum connections used are VCR (for Fujikin Valves), CF (for adapters, getters and manifold in
123 clean up) and Swagelok (for flexible tubing between modules and between ports of the cryogenic
124 separator (Swagelok 321 Stainless Steel Flexible Tubing with XBA adapter; and copper tubing).
125 Tubing and valves are 1/4" outer diameter (Swagelok) or equivalent (VCR, Fujikin). The overall
126 internal volume of the extraction line (laser-extraction, clean-up & cryogenic separation) is
127 530 cm^3. Outside the volume used for sample preparation, CF connections are used throughout. A
128 schematic overview and picture of the extraction line is provided in Figure 1.

129

130
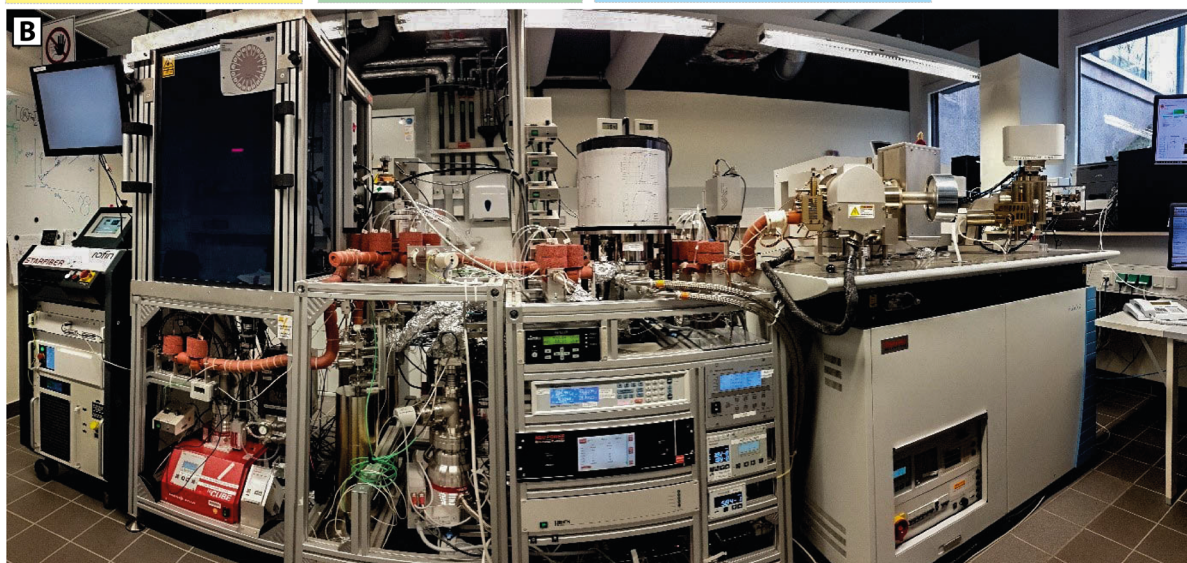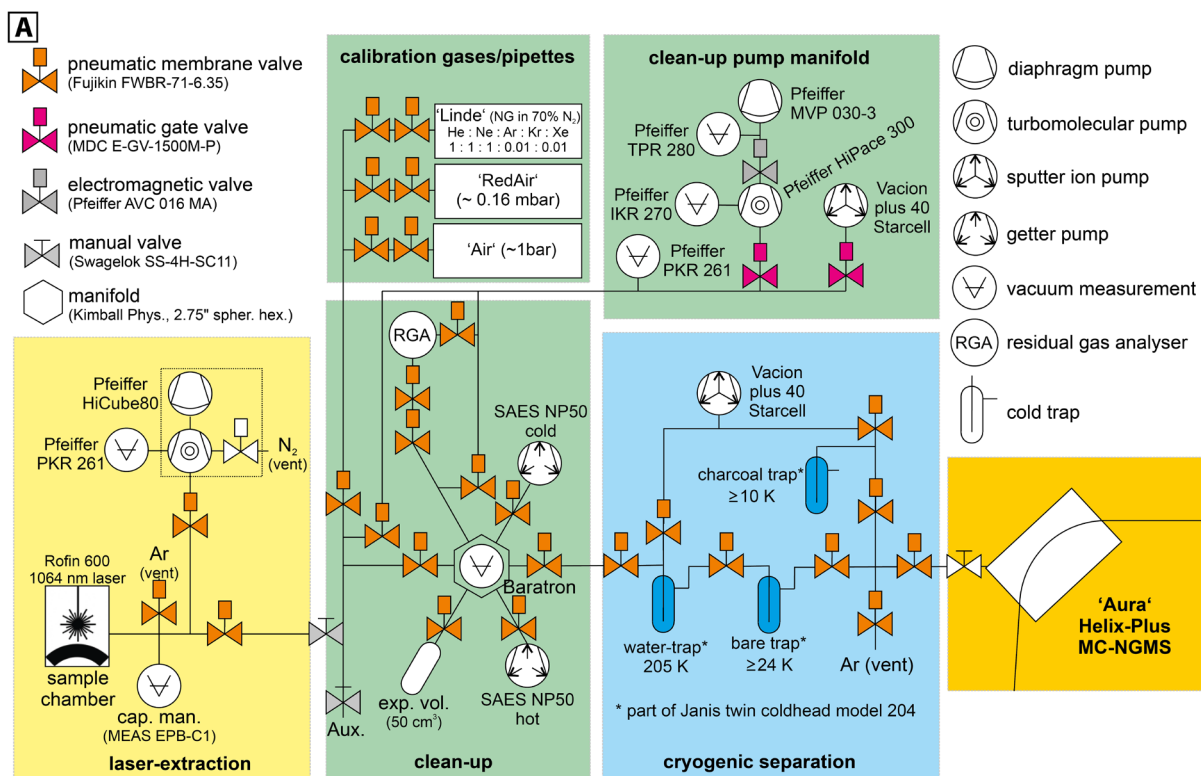
Fig. 1: (A) Schematic plan and picture (B) of the noble gas extraction and purification line at the University of Cologne. From left to right: Rofin Starfiber 600, full-protection laser-cage (laser protection windows P1P10, Laservision) housing the laser extraction, clean up unit, cryogenic separation unit and the Helix Plus NG-MCMS 'Aura'. The laboratory is temperature-stabilized to ±0.5 ºC. Further description is provided in the text.

More specifically about the individual modules:

i. Laser extraction module: Up to eighteen tungsten cups are loaded in a sample revolver, housed in a DN 200 CF flange-sandwich. The sample revolver is machined from molybdenum, which permits the heating of the tungsten cups while being situated in the revolver. To minimize

141 heat-loss through conduction, the cups sit on shards of zirconia (synthetic, cubic-stabilized
142 ZrO_2). The tungsten cups can hold up to ~600 mg quartz. The tungsten cups are reused. When
143 analysing quartz, tungsten cups are emptied with a suction micropicker (Micropicker MPC100;
144 VU Amsterdam), while remaining in the sample revolver. In cases where samples are melted
145 during extraction, tungsten cups could be cleaned in HF (then of course outside the revolver).
146 For sample loading the volume containing the revolver is vented and continuously flushed with
147 high-purity nitrogen. During laser extraction the pressure is monitored (MEAS EPB-C1 sensor,
148 welded into a male VCR connector; Disynet), in case of an eventual failure of the viewport, the
149 extraction volume is automatically purged with Argon. Energy for the heat-extraction is
150 provided by an output-tuneable 600 W fiberlaser (Rofin StarFiber600) at 1064 nm wavelength
151 through galvanometer scanner optics (Rofin RS S 14 163/67 0°) and a sapphire viewport (Kurt
152 Lesker, VPZL-275DUS). For neon-extraction of quartz, the cups are covered with tungsten-lids;
153 the heating occurs via scanning of the lids (scanning speed 20 cm/s; rastering a circular area
154 of 10 mm diameter) with a defocussed (~ 0.5 mm diameter) continuous wave beam with
155 100 W power for 15 min. Copper (melting point 1085 ºC), placed in the cup-assemblies, melts
156 at 80 W laser power (15 min extraction time); we assume that at 100 W laser power the
157 internal temperature is ≥1200 ºC. The temperature of the top of the tungsten lids is monitored
158 with a pyrometer (CellaTemp PA 29 AF 2/L; Keller HCW). The laser extraction has a dedicated
159 pumping unit (Pfeiffer HiCube80). Pressures attained after sample loading and heating of the
160 revolver (via short-term laser-heating – stepwise increased to 200 W - of an empty tungsten
161 cup; the external housing flanges reach ~50 ºC during this treatment; temperatures in adjacent
162 cups in the revolver stay below 156.6º C, which was verified with Indium wire) are usually
163 $<5*10^{-9}$ mbar (the lower limit of the pressure gauge used) after one night of pumping. Typical
164 blanks, obtained via heating of an empty tungsten cup assembly, are ~0.3 fmol Neon. A detailed
165 description of this novel laser-furnace will be provided elsewhere.
166 ii. Calibration gas pipette module: The gas-pipettes are assemblies of male and female versions
167 of pneumatically actuated Fujikin diaphragm valves (MEGA-M LA; FWB(R)-71-6.35); the
168 reservoirs were manufactured by Caburn-MDC, the insides of the reservoirs are
169 electropolished. We currently have three different gases available for noble gas calibration
170 ('Linde', 'Air', 'RedAir'). 'Linde' is a noble gas mixture in nitrogen (9.889 ± 0.009% He,
171 10.00 ± 0.01% Ne, 10.01 ± 0.01% Ar, 0.00987 ± 0.0003% Kr; 0.01023 ± 0.00002% Xe; all
172 uncertainties are ±2σ; remainder N_2; prepared gravimetrically by Linde; values as certified by
173 Linde according to DIN ISO 6141) the He is enriched in [3]He (12.3 ± 0.3 R_a; ±2σ; value as certified
174 by Linde according to DIN ISO 6141), the remaining noble gases have atmospheric
175 composition. We assume that the cryogenically purified atmospheric gases used by Linde were
176 not fractionated during this process; we have verified this for Ne within the limits of

177   uncertainties reported in this paper. 'Air' is a reservoir of air at atmospheric pressure and
178   'RedAir' a reservoir of air at reduced pressure (lab-name 'RedAir' is the abbreviation of that
179   fact). For the neon determinations we utilize 'RedAir'. The volumes of all reservoirs and the
180   pipettes have been determined relative to a gravimetrically calibrated gas volume (an
181   assembly of a Swagelok SS-4H valve and a Swagelok SS-4CS-TW-50 miniature cylinder;
182   repeatedly weighed (Satorius MSA524P-1000-DI; the balance was calibrated prior to
183   calibration of the reference volume) under vacuum and filled with air at a temperature (n=16),
184   pressure and relative humidity measured with traceable and/or certified sensors
185   (thermometer: testo 110; manometer: Greisinger GMH 3181-12, DKD certificate D19853, D-K-
186   15070-01-01; hygrometer: VWR traceable 628-0031); reference volume is 51.37±0.18 cm^3
187   (±1σ). All other volumes (piping of the calibration gas filling line; pipettes and reservoirs) were
188   determined by taking pressure readings (MKS Baratron, Type 628FU5TCF1B) from repeated
189   step-wise expansion of gases. The temperature in the room where these calibrations were
190   conducted was stable to ±0.5 ºC over the course of the calibrations. The thus determined
191   volumes of the reservoir and pipette of 'RedAir' are 8740 ± 35 cm^3 and 1.457 ± 0.006 cm^3 (±1σ),
192   respectively. For filling of the 'RedAir' reservoir one pipette volume of air was expanded into
193   the reservoir; the temperature, pressure and humidity at the time of filling of the pipette were
194   measured with a traceable and certified sensor (same as above). The first pipette volume
195   extracted from the 'RedAir' reservoir contained 4.020 ± 0.027 x 10^{-9} cm^3 (±1σ) atmospheric
196   neon at standard temperature and pressure (179 ± 1 fmol atmospheric neon; ±1σ).
197 iii. Clean-up module ('Sputnik', lab-name, referring to the shape and protrusions of the central
198   manifold and its faint resemblance to the first satellite). Arranged around a central hexagonal
199   8-port manifold (Kimball Physics, 2.75" spherical hexagon) are the sample/calibration inlet,
200   the pumping outlet, a pipette leading to a residual gas analyser (Hiden HAL/3F PIC), two SAES
201   NP50 getters (one operated hot; heating current 1.6 A; ~300 ºC), the other at room
202   temperature; getters are housed in SAES GP 50 W2F bodies; water cooling is optional, not used
203   during sample analysis), an optional expansion volume, an internally heated capacitance
204   manometer (MKS Baratron, Type 628FU5TCF1B; @ 100ºC) and the outlet to the cryogenic
205   separation unit (Fig. 1). The sample/calibration inlet tubing has an auxiliary port, which e.g., is
206   used for the crushing extraction module (build around a T4S crushing unit, VU Amsterdam).
207   The clean-up module is pumped via a manifold connected through gate-valves (MDC E-GV-
208   1500M-P) to a turbopump (Pfeiffer HiPace 300; backed by a membrane pump, Pfeiffer MVP
209   030-3) and an ion pump (Agilent, Vacion 40 plus Starcell).
210 iv. Cryogenic separation module: Centre of this module is a double-cold trap unit (Janis, twin
211   coldhead model 204) that has inlet and outlet lines to three traps: a watertrap (operated at
212   205 K) a bare steel trap (≥24 K) and a charcoal trap (≥ 10 K). The cold trap unit is controlled

213   by a Lakeshore 336 Controller (Cryotronics). This module is pumped by an ion pump (Agilent,
214   Vacion 40 plus Starcell).

215

216   The performance of the bare cold trap unit for He, Ne, Ar-separation was calibrated using the
217   Residual Gas Analyser (Hiden HAL/3F PIC). Neon is quantitatively adsorbed on the bare trap at
218   24 K (>99.9985 % is adsorbed at 24 K; Fig. 2), in equilibrium about 60% of the helium is adsorbed
219   at 24 K. We use this to separate helium from neon. Helium is removed (distilled-off in
220   disequilibrium) either to the ion pump or the 10 K charcoal head, the latter if the He is to be
221   retained for analysis. Neon is fully released from the bare trap at 80 K, at this temperature argon
222   is quantitatively retained on the bare trap, permitting quantitative separation of the two gases
223   (Fig. 2).
224   Besides its functionality to separate noble gases from each other the bare trap serves as coldtrap
225   during Ne-analysis (held at 80 K) and replaces a liquid nitrogen cooled trap, which would
226   otherwise customarily be used for this purpose. The latter may introduce intensity fluctuations
227   during analysis due to changing coolant level, which we avoid with our setup. The last
228   pneumatically actuated valve before the Helix-Plus MCMS serves as inlet valve, the manual valve
229   of the Helix-Plus MCMS is permanently open.
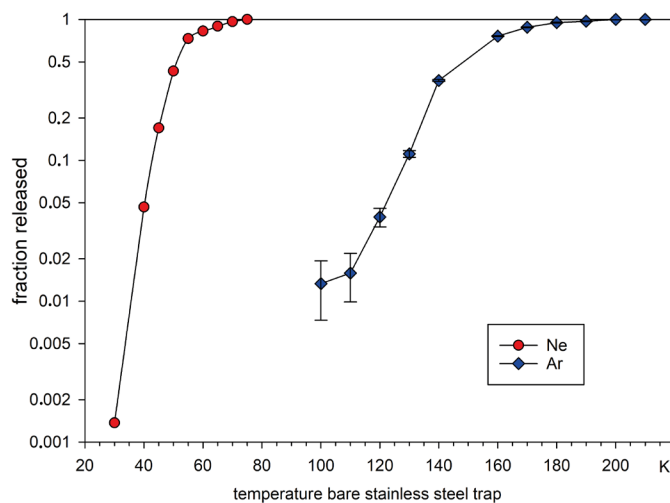
230

231   *Fig. 2: Desorption curves of Ne and Ar on the stainless-steel cold trap measured with the Hiden*
232   *Quadrupole. The uncertainties of the argon determinations at low fractions released are due to a*
233   *significant Ar-background of the quadrupole (e.g., measurement at 100 K was just 5% higher than*
234   *the background).*

235   **2.3 Automation**

236   The extraction and purification line can either be operated manually, via a switchboard for the
237   pneumatic valves and the components' original controllers, or automatically via LabView. Manual
238   operation is mainly used for development of analytical routines, automatic operation generally

for sample and calibration-gas analysis. Automatic operation liberates the operator from conducting necessarily repetitive tasks, thus helps to prevent mistakes and inconsistencies from oversight or negligence; it allows to conduct gas purification and separation under precisely identical conditions. The latter is also assisted by avoiding liquid coolants, which commonly are affected by variable coolant levels (unless automatically filled with a suitably precise system or an experienced and conscientious operator). Currently the laser system is operated manually (due to safety regulations); all subsequent steps - until admission of the gas to the mass spectrometer - are automated utilizing LabView (Version 2018) in a Windows 10 environment. The mass spectrometry analysis of the purified gas is conducted with Qtegra (Thermo Fisher Scientific).

Valve control electronics were developed and implemented in-house, including digital input/output modules (I/O modules from National Instruments) and RS-232 communication. Main devices such as, SAES getter control, Lakeshore Cryo-Controller, turbo and ion pumps offered already LabView compatible Sub-VI's (Virtual Instrument, program codes), which were implemented into the operation VI. The Agilent Ion Pump Control connection via the computer interfaces were written/developed in-house.

The gauges and controllers of the Turbo pumps (Pfeiffer) and Ion pumps (Agilent) are monitored via the operation VI. Automatic safety protocols are implemented to protect the extraction line and equipment against sudden pressure increases. Temperature setting and monitoring of the three cold traps (Janis Cryostat) is performed by the Lakeshore 336 controller, which in turn is controlled via the operation VI.

LabView computing of the extraction sequence/protocol was programmed in single commands and steps, joined into command sequences connected in series as sub-VIs for each extraction protocol (various noble gases and sources of samples or calibration gas). Pressure and temperature control sequences are programmed in continuous loop to ensure stability and safety during operation. For handling, a structured user interface was designed (Fig. 3), which provides the user with information about all parameters, total duration, and additionally logs every extraction step.

266
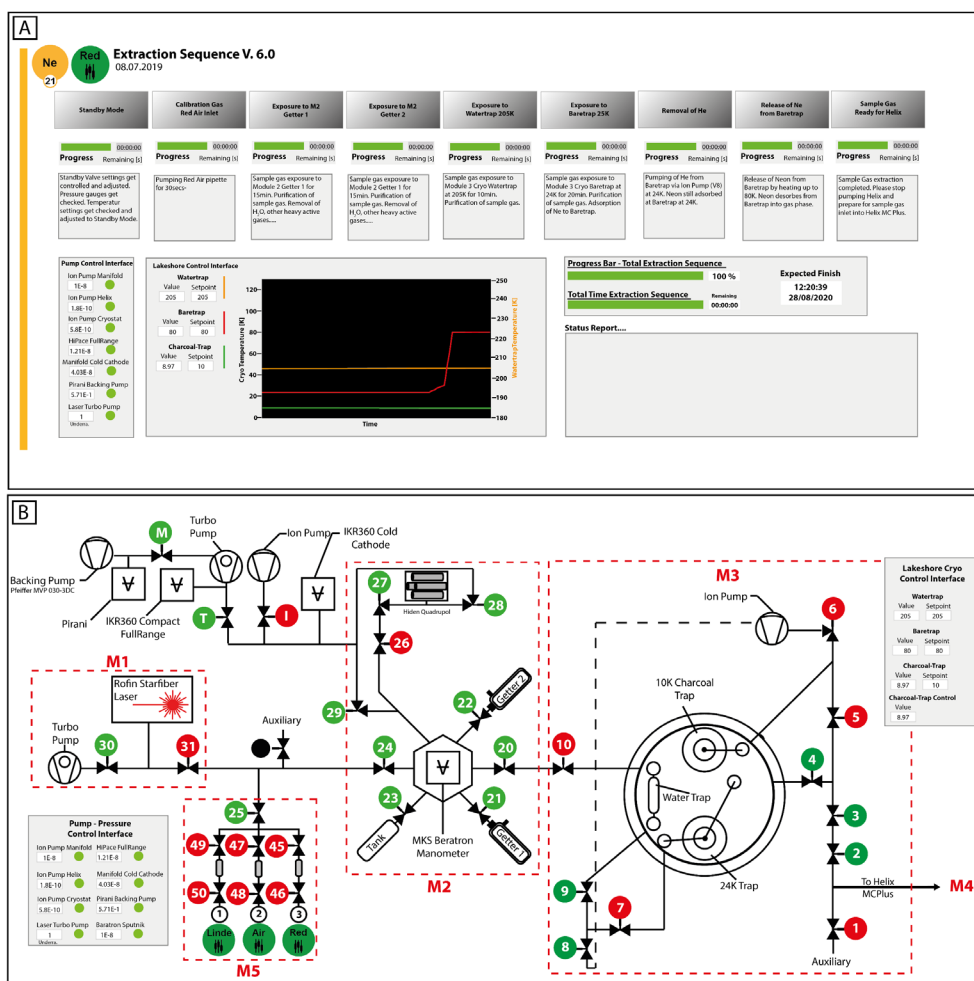
Fig. 3: Screenshots of the operating VIs of the Cologne Noble Gas Helix MCPlus. (A) The Neon VI
informs the user in real time about current data, such as pressure and temperature, as well as about
the current status of the preparation(B) Valve circuit overview.

3. Analytical Procedure

Quartz samples are cleaned using standard procedures using dilute HF as etchant (Kohl and
Nishiizumi, 1992). Up to 600 mg of quartz are loaded into tungsten-cups and covered with a
tungsten-lid, the latter has a small hole to facilitate gas release. When opening the laser furnace
for re-loading, the furnace is vented and purged with a continuous flow of pure nitrogen. In normal
operation, after the initial installation and bake-out, the internal parts of the furnace are never
again exposed to air. The tungsten cups and lids remain in the nitrogen atmosphere during sample
(re-)loading. Cups are emptied with a suction micropicker (Micropicker MPC100, VU Amsterdam)
while seated in the revolver, and weighed samples are transferred from the glass vials into the
cup through a miniature metal funnel (glass funnels produced undesirable static effects). After
reloading, the sample revolver is heated by firing the laser on an empty cup; pressure $<5*10^{-9}$
mbar is usually achieved after pumping overnight. During this clean-up, and during subsequent
analyses, the temperature of adjacent cups does not exceed 156.6 ºC (verified with Indium wire).

283   Cosmogenic Ne is extracted from quartz by heating the sample with a defocussed laser beam at
284   100 W for 15 min; at these settings, the cup-insides reach ~1200 °C. This temperature allows
285   reliable extraction of cosmogenic neon (Vermeesch et al., 2015). After heating the furnace, it is
286   allowed to cool for five minutes before the sample is expanded to the clean-up module.

287   For calibrations, the calibration gas is expanded for 30 sec into the pipette, the pipette volume is
288   then expanded into the clean-up volume. After this step, purification is identical for sample and
289   calibration gases. The pipetting of calibration gas, and the purification of sample and calibration
290   gases, is fully automatized.

291   Reactive gases are removed by sequential exposure to two metal getters (SAES NP50); the first is
292   operated hot, the other at room temperature. The gas is exposed to each for 15 min. Subsequently
293   the gas is exposed to the water trap at 205 K for 10 min. The remaining inert gases are exposed to
294   the bare-metal trap at 24 K for 20 min, which is then pumped for 5 min to remove helium from
295   the sample gas. The trap is then isolated and heated to 80 K, followed by five-minutes holding time
296   for re-equilibration. Neon is quantitatively released, and argon is quantitatively retained on the
297   trap. Subsequently, Ne gas is expanded into the Helix MCMS for analysis. The bare trap at 80 K
298   remains connected to the mass spectrometer during analysis, for pumping of CO_2 and Ar evolving
299   from the mass spectrometer.

300   The configuration of the Helix is described above. For maximum sensitivity and precision for
301   abundance determination (Wielandt and Storey, 2019), we use the widest (0.25 mm) source slit
302   for neon analysis. We run the source at an electron energy of 115 eV, trap current of 200 μA and
303   an acceleration voltage of 9.9 kV.

304   ^{20}Ne is measured on the high-resolution L1 Faraday cup (fitted with 10^{13} Ω pre-amplifier), fully
305   resolved from $^{40}Ar^{2+}$ and from molecular interferences such as HF^+, $H_2{}^{18}O^+$. ^{21}Ne is measured
306   off-centre on the high-resolution L1 multiplier, at a position that is free from interference from
307   $^{20}NeH^+$. ^{22}Ne is measured at peak centre on the H1 Faraday cup (fitted with 10^{13} Ω pre-amplifier);
308   interference from $CO_2{}^{2+}$ is corrected via monitoring of the double/single-charged ratio of CO_2
309   in-between samples and measurement of CO_2 during sample analysis, which we found to be stable
310   at 0.0437 ± 0.001 for our system throughout the period for which the data we report here were
311   obtained. The corresponding corrections of ^{22}Ne intensities are < 0.3 % for one shot of 'RedAir'
312   calibration gas (~17 fmol ^{22}Ne). The uncertainties of the correction are ~2 %, which add < 0.006%
313   uncertainty to the intensity determinations for 'RedAir'. These values scale linearly for smaller or
314   larger amounts of ^{22}Ne as found in samples. $CO_2{}^+$ is measured on the Faraday cup of the Axial
315   collector (fitted with 10^{13} Ω pre-amplifier). We refrain from analysing the larger Neon-beams
316   (^{22}Ne, ^{20}Ne) on the multipliers, since we found that they are a significant source of CO_2 upon being
317   hit by beams larger than those typical for ^{21}Ne signals (for analysing blanks, however, we use a

318   multiplier for ^{20}Ne and ^{22}Ne). Besides, the Faraday cups have a superior linearity and stability over

319   time (Wielandt and Storey, 2019). The mass spectrometer sensitivity, mass-discrimination and

320   multiplier vs. Faraday gain is calibrated with 'RedAir', which is measured at least once a day during

321   sample runs. Each batch of samples includes at least one measurement of ~100 mg CREU-1

322   (Vermeesch et al., 2015) to monitor the performance of the extraction and purification system.

323   We are in the process of producing a new intercomparison material to replace CREU-1, whose

324   supplies are limited and eventually will run too low for regular use.

4. Performance

326   The within-run reproducibility of Neon-isotope ratios as determined for calibration gas ('RedAir',

327   ~ 17 fmol atmospheric Ne) is similar for ^{21}Ne/^{20}Ne and ^{22}Ne/^{20}Ne ratios, with 0.46 % and 0.37 %

328   ($\pm1\sigma$, n=52), respectively. This dispersion is larger than the uncertainty of individual

329   measurements (Fig. 4); this feature, and the values for dispersion, are similar to those reported

330   for other Helix Plus instruments (Honda et al., 2015; Wielandt and Storey, 2019). The second

331   measurement period, with the increased uncertainties of the ^{21}Ne/^{20}Ne ratios, was performed

332   after an extended period of development work for other noble gas isotopes. We use the means

333   and the uncertainty of the means of calibrations within runs to calibrate the measurements

334   samples, i.e., propagate the observed dispersion in calculations of the abundance of cosmogenic

335   ^{21}Ne in samples. Derived $^{21/20}$Ne and $^{22/20}$Ne ratios of 22 aliquots of CREU-1, including five power

336   step extractions (Table 1), reveal a spallation line of 1.078 ± 0.022 ($\pm2\sigma$), which is

337   indistinguishable from the published value of 1.108 ± 0.014 ($\pm2\sigma$; Vermeesch et al., 2015, Fig. 5).

338   The calculated cosmogenic ^{21}Ne abundances from 22 aliquots of CREU-1 (Table 1) all agree within

339   2σ with their arithmetic mean ($348 \pm 10 * 10^6$ atoms/g; $\pm2\sigma$); thus, we may calculate an error-

340   weighted mean: $348 \pm 2 * 10^6$ atoms/g ($\pm2\sigma$), which is indistinguishable from the published value

341   ($348 \pm 10 * 106$ atoms/g; Vermeesch et al., 2015, see Fig. 6). We conclude that the reproducibility

342   and accuracy of the current set up at the University of Cologne for determining cosmogenic ^{21}Ne

343   in quartz is similar to or better than those reported for other laboratories worldwide (Vermeesch

344   et al., 2015, Fig. 6; Farley et al., 2020; Ma et al., 2015).

345
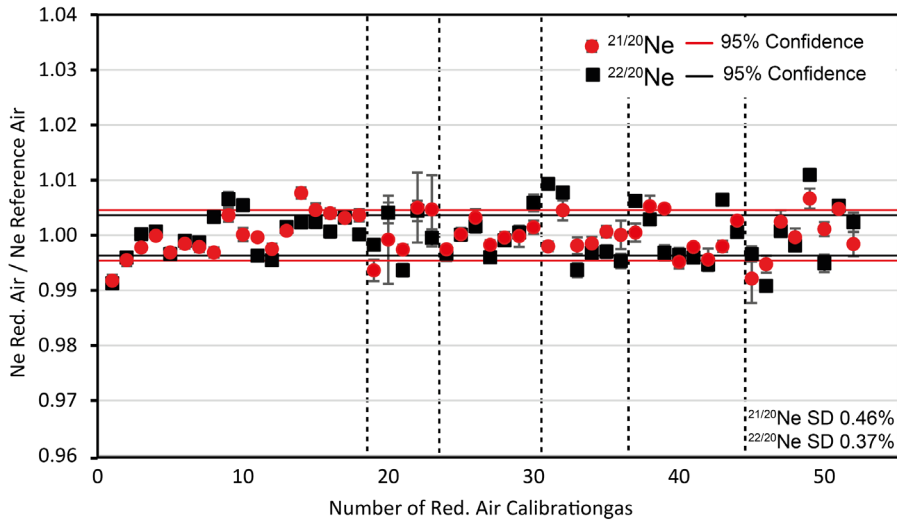
Fig. 4: Reproducibility of standard gas 'RedAir' measurements for sample runs, during the period between March 2020 and December 2020. Isotopic ratios are normalized to air for each run (mean of isotope ratios obtained in run/atmospheric ratio). Stippled black lines delineate individual runs. Error bars on individual data points are ±1σ. Symbol size is commonly larger than the corresponding error bars, which may therefore be hidden.

346
347
348
349
350

351
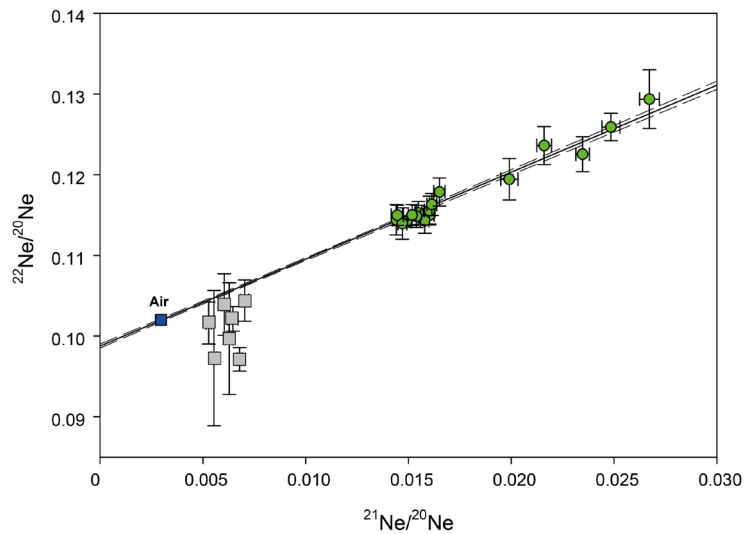
Fig. 5: Neon-three-isotope plot for CREU-1 intercomparison material measured in Cologne. Error bars are ±1 σ. The cloud of green symbols displays single-step CREU extractions (100 W-15 min), the green dots to the right of the cluster are the initial heating steps of stepwise extractions (at varying laser output), grey rectangles are the subsequent steps that invariably had low abundance; for details see Table 1. Data of samples depicted in green are included in the regression calculation; data of the grey rectangles are excluded. The slope of the regression of the data (forced through air) is 1.078 ± 0.022 (±2σ), which is indistinguishable from the published value of 1.108 ± 0.014 (±2σ; Vermeesch et al., 2015). The dotted line denotes the 95% confidence interval.

352
353
354
355
356
357
358
359
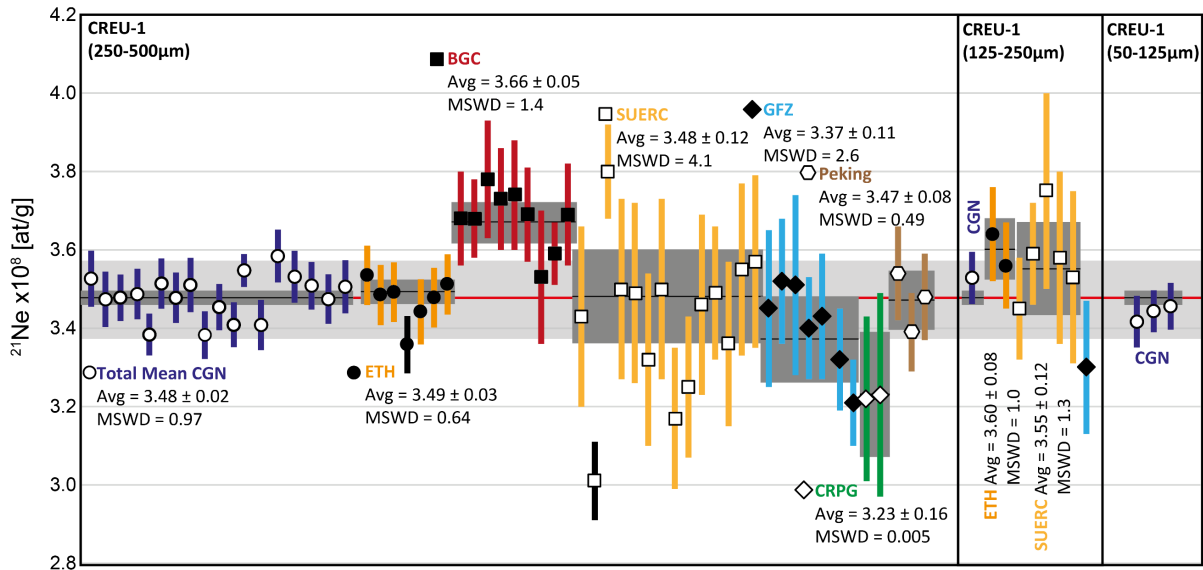
360

361 *Fig. 6: Compilation of CREU-1 ²¹Ne concentrations (±2σ uncertainties) measured at Cologne (CGN),*

362 *compared to reported ²¹Ne concentrations from interlaboratory comparison from Vermeesch et al.*

363 *(2015) and data from the Peking noble gas lab from Ma et al. (2015). Black bars were considered*

364 *outliers by the original authors and not used for calculation of averages (Vermeesch et al., 2015).*

365 *The data is divided into three sections, each for a different CREU-1 grain-size analysed. The average*

366 *²¹Ne concentration for CREU-1 of 3.48 ± 10 * 10⁸ at/g reported by Vermeesch et al. (2015) is marked*

367 *as light-grey band and a red line for the mean. Lab-individual error-weighted means are displayed*

368 *as black lines with their respective uncertainty in dark grey. The average obtained for CREU-1 at*

369 *Cologne (all grain-sizes, n=22) is 3.48 ± 0.02 * 10⁸ at/g (±2 σ; error-weighted standard deviation).*

370 *The MSWD values (Mean Square of the Weighted Deviates ('reduced Chi-square', Mcintyre et al.*

371 *(1966)) are reported for all individual laboratory-means (Vermeesch et al., 2015; this study). CGN =*

372 *University of Cologne, ETH = Eidgenössische Technische Hochschule Zürich, BGC = Berkeley*

373 *Geochronology Center, SUERC = Scottish Universities Environmental Research Centre Glasgow, CRPG*

374 *= Centre de Recherches Pétrographiques et Géochimiques Nancy, GFZ = Deutsches*

375 *GeoForschungsZentrum Potsdam.*

376 Table 1: CREU Data

Sample ID	Mass [g]	Extraction Power [W]	²⁰Ne [10⁹ at/g]			21/20			22/20			²¹Ne* [10⁶ at/g]		
01_CREU1 250-500µm	0.0997	100	30.97	±	0.15	0.01434	±	0.00014	0.11381	±	0.00129	352.7	±	3.6
02_CREU1 250-500µm	0.0993	100	29.81	±	0.24	0.01461	±	0.00015	0.11415	±	0.00129	347.4	±	3.5
03_CREU1 50-125µm	0.1038	100	24.89	±	0.15	0.01669	±	0.00012	0.11646	±	0.00170	341.7	±	3.3
04_CREU1 50-125µm	0.1319	100	25.73	±	0.20	0.01634	±	0.00018	0.11727	±	0.00089	344.4	±	2.7
05_CREU1 50-125µm	0.1179	100	24.86	±	0.17	0.01686	±	0.00017	0.11614	±	0.00130	345.6	±	3.0

Sample				±			±			±			±	
06_CREU1 125-250µm	0.1078	100	27.00	±	0.35	0.01603	±	0.00022	0.11499	±	0.00110	352.9	±	3.3
07_CREU1 250-500µm	0.1210	100	29.13	±	0.36	0.01490	±	0.00021	0.11417	±	0.00065	347.8	±	3.0
08_CREU1 250-500µm	0.1105	100	30.46	±	0.25	0.01441	±	0.00018	0.11443	±	0.00189	348.7	±	3.2
09_CREU1 250-500µm	0.1312	100	26.37	±	0.32	0.01579	±	0.00021	0.11428	±	0.00153	338.4	±	2.7
10_CREU1 250-500µm	0.1128	100	29.92	±	0.40	0.01470	±	0.00022	0.11395	±	0.00195	351.4	±	3.2
11_CREU1 250-500µm	0.1113	100	26.60	±	0.33	0.01603	±	0.00026	0.11556	±	0.00179	347.8	±	3.2
12_CREU1 250-500µm	0.1053	100	30.56	±	0.36	0.01445	±	0.00030	0.11498	±	0.00125	351.1	±	3.5
13_CREU1 250-500µm	0.1125	100	27.01	±	0.24	0.01548	±	0.00017	0.11526	±	0.00143	338.3	±	3.0
14_CREU1 250-500µm	0.1210	100	26.21	±	0.30	0.01614	±	0.00024	0.11632	±	0.00137	345.4	±	3.0
15_CREU1 250-500µm	0.1252	100	25.16	±	0.19	0.01651	±	0.00027	0.11786	±	0.00174	340.9	±	2.9
16_CREU1 250-500µm	0.2063	100	28.54	±	0.33	0.01539	±	0.00020	0.11485	±	0.00137	354.8	±	2.1
17_CREU1 250-500µm	0.1077	100	27.90	±	0.30	0.01518	±	0.00019	0.11502	±	0.00129	340.9	±	3.2
18_CREU1 250-500µm	0.1126	30	16.44	±	0.16	0.02160	±	0.00036	0.12362	±	0.00236			
	0.1126	50	8.61	±	0.08	0.00628	±	0.00019	0.09968	±	0.00692			
	0.1126	70	5.71	±	0.05	0.00528	±	0.00013	0.10162	±	0.00260			
	0.1126	100	3.92	±	0.05	0.00554	±	0.00015	0.09727	±	0.00838	358.5	±	3.4
19_CREU1 250-500µm	0.1111	24	11.96	±	0.17	0.02672	±	0.00048	0.12936	±	0.00364			
	0.1111	100	18.06	±	0.23	0.00678	±	0.00012	0.09711	±	0.00146	353.2	±	3.3
20_CREU1 250-500µm	0.1301	24	14.27	±	0.12	0.02347	±	0.00033	0.12255	±	0.00217			
	0.1301	100	16.51	±	0.18	0.00646	±	0.00025	0.10213	±	0.00152	350.9	±	3.0
21_CREU1 250-500µm	0.1180	30	13.11	±	0.15	0.02485	±	0.00044	0.12592	±	0.00170			
	0.1180	100	14.79	±	0.09	0.00703	±	0.00020	0.10440	±	0.00256	347.5	±	3.2
22_CREU1 250-500µm	0.1075	50	18.42	±	0.12	0.01991	±	0.00042	0.11944	±	0.00256			
	0.1075	100	12.35	±	0.11	0.00604	±	0.00010	0.10391	±	0.00381	350.6	±	3.4

377

Conclusion

The performance of the set-up for Neon-isotope measurements in the new noble gas laboratory at the University Cologne permits state-of-the art analysis of cosmogenic neon. We now regularly perform analysis of samples for cosmogenic neon for our running projects; and are open to new scientific cooperations.

Author contribution:

TJD, BR, AV development of the Cologne noble gas system. TJD, BR performance experiments and tests. BR, TJD manuscript writing.

Data Availability:

The authors confirm that the data supporting the findings of this study are available within the article.

Acknowledgements:

The equipment for the noble gas mass spectrometry laboratory described in this paper was funded by Deutsche Forschungsgemeinschaft (DFG) - project number 259990027 to TJD. The performance test was conducted and funded in the framework of the Collaborative Research Center 1211 – Earth Evolution at the Dry Limit, Deutsche Forschungsgemeinschaft (DFG) - project number 268236062 – SFB 1211. Special thanks go to Dave Wanless for patient training and continuing support in mastering 'Aura'.

Declaration of interest

The authors declare that the research was conducted in the absence of any commercial or financial relationships that could be construed as a potential conflict of interest.

References

Binnie, S., Reicherter, K., Victor, P., González, G., Binnie, A., Niemann, K., Stuart, F., Lenting, C., Heinze, S., Freeman, S., and Dunai, T. J.: The origins and implications of paleochannels in hyperarid, tectonically active regions: The northern Atacama Desert, Chile, Global and Planetary Change, 185, 103083, 2020.

Dunai, T. J.: Cosmogenic Nuclides: Principles, concepts and applications in the Earth surface sciences, Cambridge University Press2010.

Dunai, T. J., Lopez, G. A. G., and Juez-Larre, J.: Oligocene-Miocene age of aridity in the Atacama Desert revealed by exposure dating of erosion-sensitive landforms, Geology, 33, 321-324, 10.1130/g21184.1, 2005.

Eberhardt, P., Eugster, O., and Marti, K.: A redetermination of the isotopic composition of atmospheric neon, Zeitschrift fuXr Naturforschung, 20a, 623-624, 1965.

Espanon, V. R., Honda, M., and Chivas, A. R.: Cosmogenic 3He and 21Ne surface exposure dating of young basalts from Southern Mendoza, Argentina, Quaternary Geochronology, 19, 76-86, 2014.

Farley, K., Treffkorn, J., and Hamilton, D.: Isobar-free neon isotope measurements of flux-fused potential reference minerals on a Helix-MC-Plus10K mass spectrometer, Chemical Geology, 537, 119487, 2020.

Gillen, D., Honda, M., Chivas, A. R., Yatsevich, I., Patterson, D. B., and Carr, P. F.: Cosmogenic 21Ne exposure dating of young basaltic lava flows from the Newer Volcanic Province, western Victoria, Australia, Quaternary Geochronology, 5, 1-9, 2010.

426 Györe, D., Tait, A., Hamilton, D., and Stuart, F. M.: The formation of NeH+ in static vacuum mass
427 spectrometers and re-determination of 21Ne/20Ne of air, Geochimica et Cosmochimica Acta, 263, 1-
428 12, 2019.
429

430 Honda, M., Zhang, X., Phillips, D., Hamilton, D., Deerberg, M., and Schwieters, J. B.: Redetermination
431 of the 21Ne relative abundance of the atmosphere, using a high resolution, multi-collector noble gas
432 mass spectrometer (HELIX-MC Plus), International Journal of Mass Spectrometry, 387, 1-7, 2015.
433

434 Kohl, C. and Nishiizumi, K.: Chemical isolation of quartz for measurement of in-situ-produced
435 cosmogenic nuclides, Geochimica et Cosmochimica Acta, 56, 3583-3587, 1992.
436

437 Ma, Y., Wu, Y., Li, D., and Zheng, D.: Analytical procedure of neon measurements on GV 5400 noble
438 gas mass spectrometer and its evaluation by quartz standard CREU-1, International Journal of Mass
439 Spectrometry, 380, 26-33, 2015.
440

441 Ma, Y., Wu, Y., Li, D., Zheng, D., Zheng, W., Zhang, H., Pang, J., and Wang, Y.: Erosion rate in the
442 Shapotou area, northwestern China, constrained by in situ-produced cosmogenic 21Ne in long-
443 exposed erosional surfaces, Quaternary Geochronology, 31, 3-11, 2016.
444

445 McIntyre, G., Brooks, C., Compston, W., and Turek, A.: The statistical assessment of Rb-Sr isochrons,
446 Journal of Geophysical Research, 71, 5459-5468, 1966.
447

448 McPhillips, D., Hoke, G. D., Liu-Zeng, J., Bierman, P. R., Rood, D. H., and Niedermann, S.: Dating the
449 incision of the Yangtze River gorge at the First Bend using three-nuclide burial ages, Geophysical
450 Research Letters, 43, 101-110, 2016.
451

452 Niedermann, S.: Cosmic-ray-produced noble gases in terrestrial rocks: dating tools for surface
453 processes, Reviews in Mineralogy and Geochemistry, 47, 731-784, 2002.
454

455 Niedermann, S., Graf, T., Kim, J., Kohl, C., Marti, K., and Nishiizumi, K.: Cosmic-ray-produced 21 Ne in
456 terrestrial quartz: the neon inventory of Sierra Nevada quartz separates, Earth and Planetary Science
457 Letters, 125, 341-355, 1994.
458

459 Ritter, B., Stuart, F. M., Binnie, S. A., Gerdes, A., Wennrich, V., and Dunai, T. J.: Neogene fluvial
460 landscape evolution in the hyperarid core of the Atacama Desert, Scientific Reports, 8, 13952,
461 10.1038/s41598-018-32339-9, 2018.
462

463 Saxton, J.: The 21 Ne/20 Ne ratio of atmospheric neon, Journal of Analytical Atomic Spectrometry,
464 35, 943-952, 2020.
465

466 Vermeesch, P., Balco, G., Blard, P. H., Dunai, T. J., Kober, F., Niedermann, S., Shuster, D. L., Strasky, S.,
467 Stuart, F. M., Wieler, R., and Zimmermann, L.: Interlaboratory comparison of cosmogenic Ne-21 in
468 quartz, Quaternary Geochronology, 26, 20-28, 10.1016/j.quageo.2012.11.009, 2015.
469

470   Wielandt, D. and Storey, M.: A new high precision determination of the atmospheric 21 Ne
471   abundance, Journal of Analytical Atomic Spectrometry, 34, 535-549, 2019.

472